23 European Conference on Fracture – ECF23

Computational semi-analytic code for stress singularity analysis

M.A. Herrera-Garrido[a,*], V. Mantič[a], A. Barroso[a]

[a]*Grupo de Elasticidad y Resistencia de Materiales, Escuela Técnica Superior de Ingeniería, Universidad de Sevilla, Camino de los Descubrimientos, s/n, 41092 Sevilla, Spain*

Abstract

Problems of stress singularities in single or multi-material corners have been addressed by many authors over the years. Most of the authors presented closed-form corner-eigenequations for special cases, and often there is no easy way to check if the solution is correct. In this work, we present a general computational tool that can solve many different cases of stress singularity problems for multi-material corners under generalized plane strain. The semi-analytic code is based on the matrix formalism presented in Mantič et al. (1997, 2014); Barroso et al. (2003); Herrera-Garrido et al. (2022) and is developed in MATLAB. The following boundary conditions are implemented: stress-free, fixed, some restricted or allowed direction of displacements (defined either in the reference frame aligned with the cylindrical coordinate system or in an inclined reference frame), or frictional sliding. The following interface condition between two consecutive materials are implemented: perfectly bonded, and frictionless or frictional sliding. The code can analyze both open and closed (periodic) corners, composed of one or multiple materials with isotropic, transversely isotropic or orthotropic (with any orientation) constitutive laws. The code has proven to be a reliable, very accurate, robust and easy-to-use tool, which has been verified by comparing the results computed with those obtained by other authors. A summary of the corner singularity problems solved is presented. The results of the corner singularity analysis obtained by the code can be further used for prediction of crack onset at the corner tip by the Coupled Criterion of Finite Fracture Mechanics and FEM, see García and Leguillon (2012) and references therein.

1. Introduction

When analyzing a structure using the finite element method (FEM), at some points called singular points, the solution obtained may be inaccurate. This is due to the fact that these points act as *stress singularities*. A stress singularity is a place where stresses are theoretically infinite in the framework of linear elasticity. In these cases, it

---

* Corresponding author.
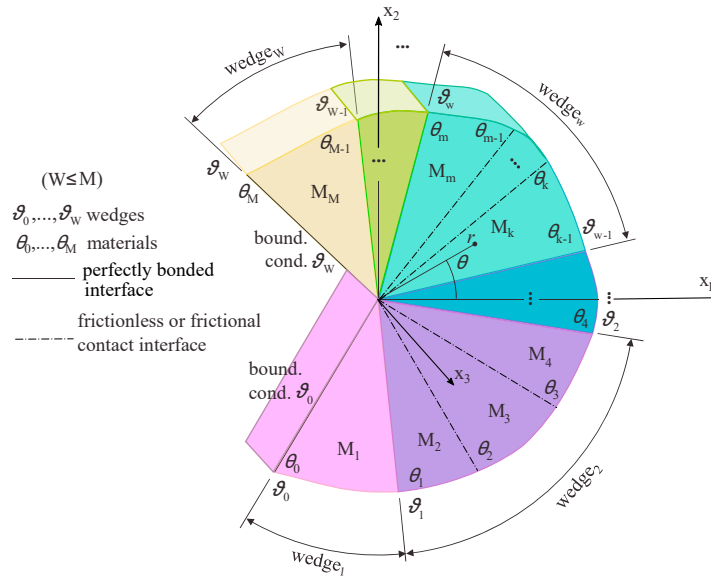 *E-mail address:* mherrera13@us.es

Fig. 1. Multi-material corner notation, 2D view.

is necessary to consider the deformation and stress field in the vicinity of these singular points to improve the FEM model.

A stress singularity can be caused by jumps in boundary conditions, geometries, or material properties, see Leguillon and Sanchez-Palencia (1987); Yosibash (2012). In this work, we present a semi-analytic code, a fast and reliable tool that can be used to study displacements and stress fields near the singular point under generalized plane strain. We refer to the singular point as a corner tip and to his neighborhood as a corner. When a corner is made of more than one material, it is called a multi-material corner. In Fig. 1, a multi-material corner is shown to illustrate the notation used. This tool includes the possibilities of studying both open and closed (periodic) corners, with one or multiple materials, with perfectly bonded interfaces or allowing the frictional or frictionless sliding and with several kinds of boundary conditions such as stress-free, clamped or allowing or restricting the displacement in one direction, covering symmetry and skew-symmetry conditions among others.

The computational semi-analytic code presented is based on the matrix formalism for a compact representation of different boundary and interface conditions in the multi-material corner introduced in Mantič et al. (1997, 2014); Barroso et al. (2003), see also Mantič et al. (2003). This formalism follows the proposal by Ting (1997), showing that for the study of the asymptotic displacement and stress fields near a singular point in anisotropic materials in a generalized plane strain state, it is convenient to employ the Stroh sextic formalism in complex variables together with a transfer matrix concept for all the single-material wedges in the corner.

2. Code structure

The code is written in Matlab using the Symbolic Math Toolbox. It is divided into six different modules:

- Data input
- Definition of single-material wedges
- Boundary and interface condition matrices
- Characteristic system assembly
- Solution of the characteristic system to compute the singularity exponents.
- Displacement and stress singular fields

2.1. Data input

The user creates, interactively or off-line, a text file defining the properties of the corner to be solved. These properties are:

- Number of materials making up the corner
- Type of corner, open or closed (periodic) corner
- For each material in the corner, indicate whether it is isotropic, orthotropic or transversely isotropic
- For each material in the corner, indicate the angular sector occupied by the material in the corner, θ_{m-1} and θ_m in Fig.1
- Depending on the selected kind of material, the following engineering constant are indicated
  - Isotropic material: the Young modulus, E, and the Poisson ratio, ν
  - Orthotropic material: nine stiffness constants, E_{11}, E_{22}, E_{33}, G_{12}, G_{13}, G_{23}, ν_{12}, ν_{13} y ν_{23}, and the angles defining the material orientation with respect to the corner coordinate system
  - Transversely isotropic material: the Young modulus E and the Poisson ratio ν in the plane of isotropy $(1,2)$, the stiffness constants associated with the the the axis of symmetry (3), the Young modulus E_{33}, the Poisson ration ν_{31} and the shear modulus G_{13}, and the angles defining the material orientation with respect to the corner coordinate system
- For an open corner: the angles and the prescribed boundary conditions for the two external faces
- For a closed corner or a multi-material open corner: the angle and the prescribed interface condition for each interface in the corner
- In case a parameterization is requested
  - Parameterization of the corner angle, indicating the number of steps and the range of angles
  - Parameterization of the orientation of any of the orthotropic or transversely isotropic materials. The number of the material in the corner, and the number of steps and the range of angles of the rotation with respect to the axis x_3.

Just by changing one of the above defined parameters, such as the parameter indicating the type of boundary condition, we can change the study of a corner with stress-free outer surfaces to the study of a clamped corner.

2.2. Definition of single-material wedges

To characterize each material, the concept of transfer matrix, $\mathbf{E}_m$, proposed by Ting (1996), is employed. This matrix relates the displacements and stress function on one face of the material with the displacements and stress function on its other face. It depends on the elastic constants and the initial and final angles of each material, θ_{m-1} and θ_m, respectively. It is based on the matrices $\mathbf{A}$ and $\mathbf{B}$ of the sextic formalism established by Stroh (1958, 1962). See Ting (1996); Barroso et al. (2003); Mantič et al. (2014); Hwu (2021); Herrera-Garrido et al. (2022) for a detailed explanation of the Stroh formalism.

2.3. Boundary and interface condition matrices

In an open corner, the boundary conditions are imposed on both outer faces in addition to the interface conditions in the case of a multi-material corner. In the case of a closed corner, interface conditions are imposed on all interfaces between materials. To apply the boundary and interface condition the code make use of the matrix formalism presented in Mantič et al. (1997, 2014); Barroso et al. (2003) and later successfully verified by many comparisons with the results of other authors in Herrera-Garrido et al. (2022). The boundary conditions available in the code are:

- Stress-free face
- Clamped face
- Displacement u_r, u_θ, u_3, or in any other given direction, restricted
- Only displacement u_r, u_θ, u_3, or in any other given direction, allowed
- Sliding with friction

and the interface conditions are:

• Perfectly bonded
• Frictionless sliding contact
• Friction sliding contact

2.4. Characteristic system assembly

Once the code has calculated all the *transfer matrices* $\mathbf{E}_m$ for each material, the transfer matrices $\mathbf{K}_w$ for each wedge of perfectly bonded material can be calculated, and with them the matrix $\mathbf{K}_{\text{corner\_ext}}(\lambda)$ that depends on the elastic properties and the geometry of all the materials that conform the corner. Additionally, with all the boundary and interface matrices the *main boundary and interface condition matrix of the corner*, $\mathbf{D}_{\text{corner\_ext}}(\boldsymbol{\vartheta}, \boldsymbol{\omega})$ is formed. Then, the *characteristic system of corner* is expressed as:

$$\mathbf{K}_{\text{corner\_ext}}(\lambda)\mathbf{D}_{\text{corner\_ext}}^{T}(\boldsymbol{\vartheta}, \boldsymbol{\omega})\mathbf{w}_{\text{corner\_PU}} = \mathbf{0}_{6W \times 1} \tag{1}$$

where the vector $\mathbf{w}_{\text{corner\_PU}}$ is the vector containing the prescribed (null) and unknown elastic variables.

2.5. Solution of the characteristic system

To solve the *characteristic system of corner*, the system (1) is reduced to

$$\mathbf{K}_{\text{corner}}(\lambda, \boldsymbol{\omega})\mathbf{w}_{\text{corner\_U}} = \mathbf{0}_{6W \times 1} \tag{2}$$

by suppressing the columns multiplied by the prescribed (null) values of the elastic variables.

In cases where friction is not considered on the boundaries and interfaces within the corner, the characteristic matrix of the system $\mathbf{K}_{\text{corner}}(\lambda)$ depends only on λ, and it is a square matrix. In this case, the eigenvalues λ of the nonlinear characteristic system of the corner are given by the roots of the determinant of $\mathbf{K}_{\text{corner}}(\lambda)$. The code applies the *Muller method*, Muller (1956), to find these roots, and shows the real part of the determinant of $\mathbf{K}_{\text{corner}}(\lambda)$ to check if there are more possible solutions, see Fig. 3.

In cases where there are one or more boundaries or interfaces with frictional contact sliding within the corner, the matrix $\mathbf{K}_{\text{corner}}(\lambda, \boldsymbol{\omega})$ depends also on the sliding angles $\boldsymbol{\omega}$ on each of these boundaries or interfaces, and it is a rectangular matrix, leading to an apparently over-determined system. In these cases there are different ways to solve the system. The method implemented in the code is solving the following system:

$$f(\mathbf{X}) = \mathbf{K}_{\text{corner}}(\lambda, \boldsymbol{\omega})\mathbf{w}_{\text{corner\_U}} = \mathbf{0} \tag{3}$$

where

$$\mathbf{X} = \begin{bmatrix} \mathbf{w}_{\text{corner\_U}} \\ \lambda \\ \boldsymbol{\omega} \end{bmatrix}. \tag{4}$$

Generally, the values of λ are searched in $0 \leq \text{Re}(\lambda) \leq 1$ range, as those characteristic exponents correspond to singular elastic solutions in the corner with unbounded stresses and strains at the corner tip but a finite elastic

Table 1. Engineering constants for the materials used in the examples studied. Shear and elastic moduli in GPa.

Material	E_1	E_2	E_3	G_{12}	G_{13}	G_{23}	v_{12}	v_{13}	v_{23}	ϕ_2
A	68.67						0.33			
B	141.3	9.58	9.58	5	5	3.5	0.3	0.3	0.32	ϕ
C	137.9	14.48	14.48	4.98	4.98	4.98	0.21	0.21	0.21	ϕ
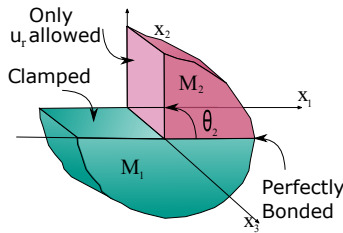
Fig. 2. Scheme of the geometry and boundary conditions used in the examples in Sections 3.1 and 3.3.

strain energy. Values of the sliding angles ω are searched in the range $-180^\circ \geq \omega \geq 180^\circ$. Remark that one ω value should be found per each interface or boundary face where the frictional sliding is imposed. To help finding a good initial point to solve the nonlinear system, a map of the minimum singular value σ_{min} given by the singular value decomposition (SVD) of the matrix $\mathbf{K}_{corner}(\lambda, \omega)$, as the one shown in Fig. 5, is displayed. In this kind of graph the darker values correspond with the lowest values, thus the possible solutions of the system.

2.6. Singular stress and displacement fields

Once the singular exponent λ, and in the presence of friction contact also the vector of sliding angles ω, are known, the values of stresses and displacements as functions of the polar angle θ for a fixed radius $r = 1$ can be computed and are shown in a plot, see an example in Fig. 6.

3. Code features and numerical results

This section will show the main functions of the semi-analytic code based on the resolution of some relevant cases. The materials defined in Table 1 are used in the examples studied. Material *A* is an isotropic material, while *B* and *C* are orthotropic materials. The last column in the table, ϕ_2 represents the angle with respect the x_1-axis of the fibres that lay in the plane $x_1 - x_3$ of the orthotropic material. In the examples shown, for simplicity, only the angle ϕ_2 has been employed, but also the angle that the fibres have with respect the other two axes can be modified.

3.1. Detection of the number of singular exponents in a range

When no frictional contact is prescribed neither as boundary condition or as interface condition, the characteristic matrix of the corner is a square matrix and its determinant can be computed. Thus, the real part of this determinant can be plotted versus λ. At a glance, the number of roots the determinant has in an interval of λ can be known, and therefore the number of possible singularity exponents of the problem. Furthermore, in these cases the argument principle can be applied, and it will inform us if there is any complex root that has not been detected by a simple observation of the real part of the determinant. In Fig. 3 the real part of the determinant of the characteristic corner of the problem shown in Fig. 2 is represented for $\theta_2 = 163^\circ$. Material *B* is used in this example both as M_1 and M_2. M_1 has the fibres parallel to the x_1 axis and the fibres of M_2 are positioned at 45° from x_1 axis. It can be seen that there are 2 real roots and possibly 1 complex root and its conjugate. This has been checked with the argument principle. In section 3.3 and in Fig. 4, these values are shown together with the solution of the same problem with different corner angles.
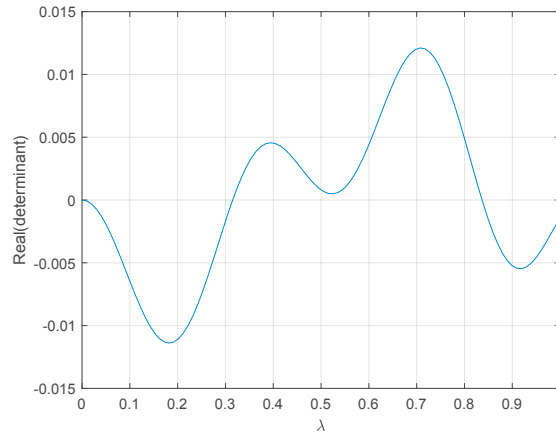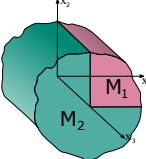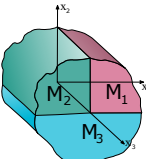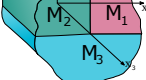
Fig. 3. Real part of the determinant of the characteristic matrix of the corner in Fig. 2 with $\theta_2 = 163°$.

Table 2. Singularity exponents and the computing time for closed multi-materials corners with all the interfaces perfectly bonded.

Example	Schema	Mat.1	Mat.2	Mat.3	Results	Computing time (sec.)
1.1		A	C $\phi_2 = 0°$		0.780303329 0.800494545	8.9
1.2		A	C $\phi_2 = 30°$		0.791201852 0.826334613	15.1
1.3		A	C $\phi_2 = 0°$	C $\phi_2 = 90°$	0.780303329 0.819782705	10.9
1.4		A	C $\phi_2 = 30°$	C $\phi_2 = 60°$	0.790798278 0.827339124	30.1

3.2. Computation of singularity exponents

In this section the numerical values of the singularity exponents for the studied examples of closed corners are presented. A closed corner is a union of single-material wedges with no outer boundary faces, thus including only interfaces between materials. The calculation of the singularity exponents for some specific cases may be used to verify closed-form formulas for λ or corner eigenequations previously developed for specific corner singularity problems by other authors, and also to improve the numerical results by FEM. In Tables 2 and 3, the singularity exponents together with the computing times are presented for some examples. For reference, the calculations were performed with a laptop DELL Precision 5550, Intel Core i9 with 16GB RAM.

In Table 2, the singularity exponents for some studied cases of closed corner with all the material perfectly bonded are presented. The difference between Examples 1.1 and 1.2 and between Examples 1.3 and 1.4, is that in Examples 1.1 and 1.3 the materials are orthotropic with the fibres in the axis x_1 or x_3, while the materials in Examples 1.2 and 1.4 are orthotropic materials with their fibres lying in the plane $x_1 - x_3$.

By modifying only one parameter in the input data, the type of interface condition, the examples in Table 2 change to the ones shown in Table 3 that represent a closed frictionless interfacial crack between the materials that were perfectly bonded in the previous examples. In this case, the interface that has been debonded is the one with $\theta = 0°$. Noteworthy, the code allows to debond any of the interfaces, even all of them.

For more numerical examples solved with this semi-analytic code, see Herrera-Garrido et al. (2022).

Table 3. Singularity exponents and the computing time for closed corners with one interface with frictionless sliding and the remaining interfaces perfectly bonded.

Example	Scheme	Mat.1	Mat.2	Mat.3	Results	Computing time (sec.)
2.0		A			0.5	2.2
2.1		A	C $\phi_2 = 0°$		0.390151665 0.488207107 0.882007602	19.4
2.2		A	C $\phi_2 = 30°$		0.397478163 0.480719195 0.876622817	34.5
2.3		A	C $\phi_2 = 0°$	C $\phi_2 = 90°$	0.390151665 0.496862211 0.887884755	26.2
2.4		A	C $\phi_2 = 30°$	C $\phi_2 = 60°$	0.379533452 0.488120275 0.881144785	37.8

3.3. Parameterization

The semi-analytic code allows the user to carry out a parameterization study of the dependence of the singularity exponent on some of the variables of the corner problem. In Fig. 4, the singularity exponents are plotted versus the solid angle θ_2 of a wedge that is bonded to a semi-plane, see Fig. 2.The real part of λ is given by solid lines, while the imaginary one is drawn with a dashed line. The imaginary values of λ correspond to the real part of λ represented with the same color. From all the possible boundary conditions presented in Section 2.3, in this example the outer boundary of semi-plane is clamped while on the wedge boundary only the displacement in the radial direction is allowed. Material C with $\phi_2 = 0°$ is used for the semi-plane and with $\phi = 45°$ for the wedge. Starting with $\theta_2 = 10°$ it can be seen that there are 3 real roots between 0 and 1. For the studied values of θ_2 between 100° and 140°, 4 real roots in the same range have been found. While for the studied values of $\theta_2 > 140°$ 2 real roots and 1 pair of complex conjugate roots have been found.

3.4. Determination of the number of singularity exponents and computation of sliding directions

In the case that a frictional contact is prescribed, either as a boundary or interface condition, a map of the minimum singular value σ_{min} of the corner characteristic matrix is plotted versus λ and ω, the singularity exponent and the sliding angle, respectively, see an example in Fig. 5. When σ_{min} is 0 for a given pair (λ, ω), it means that this combination of values of λ and ω is a solution of the problem. In Fig. 5, the lowest values of σ_{min} are represented with dark blue color, thus the possible solutions of the characteristic system must be searched for (λ, ω) pairs corresponding to the darkest points. The case studied here is a single-material wedge of solid angle 300°, at $\theta_0 = 0°$ the boundary condition is sliding with a frictional coefficient $\mu = 1$ and the boundary at $\theta_1 = 300°$ is clamped. The material used is material A in Table 1. It can be seen that this problem has 11 solutions, once they all are found it can be checked for which of them the energy dissipation condition due to friction is fulfilled.

3.5. Displacements and stresses

The last functionality presented is the possibility to represent the singular stress and displacement fields of the corner. In Fig. 6 the stress and the displacement fields for the singularity exponent $\lambda = 0.61028006$ with $\omega = 199.96°$, the solution for a wedge of solid angle 90° that slides with a frictional coefficient $\mu = 0.5$ over a semi-plane are

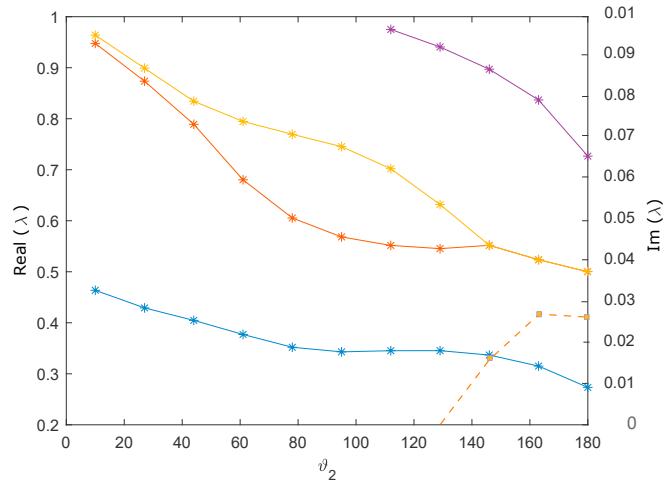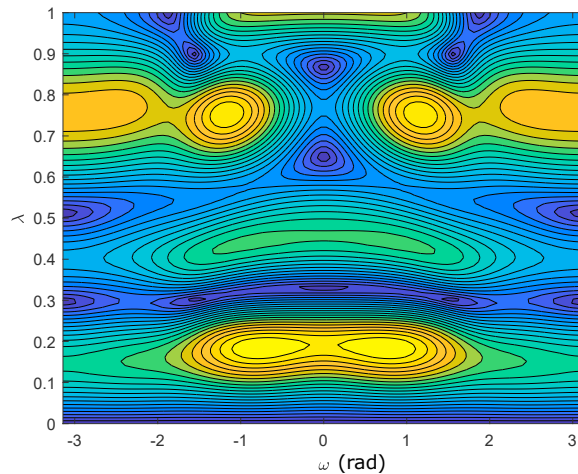Fig. 4. Singularity exponents versus the wedge angle θ_2, see Fig. 2 for reference.

Fig. 5. Minimum singular value, $\sigma_{\min}$, of the corner characteristic matrix for (λ, ω) pairs for the case of a single-material wedge of solid angle $300°$

represented. The material used for the example is the material B with $\phi_2 = 90°$ for the semi-plane and $\phi_2 = 0°$ for the wedge. The boundary conditions at both outer faces are stress free.

4. Conclusion

The developed general purpose semi-analytical code has proven to be an efficient and accurate computational tool that can be very useful for both researchers and engineering companies that have to simulate by FEM their structures including discontinuities in boundary conditions, geometry or material properties. In Herrera-Garrido et al. (2022), the code has already demonstrated that its results are extremely accurate thanks to the comparison with the analytical results obtained by other authors using more specific methods. In this work the capabilities and variety of functions of this code and all the information the code can provide have been shown.
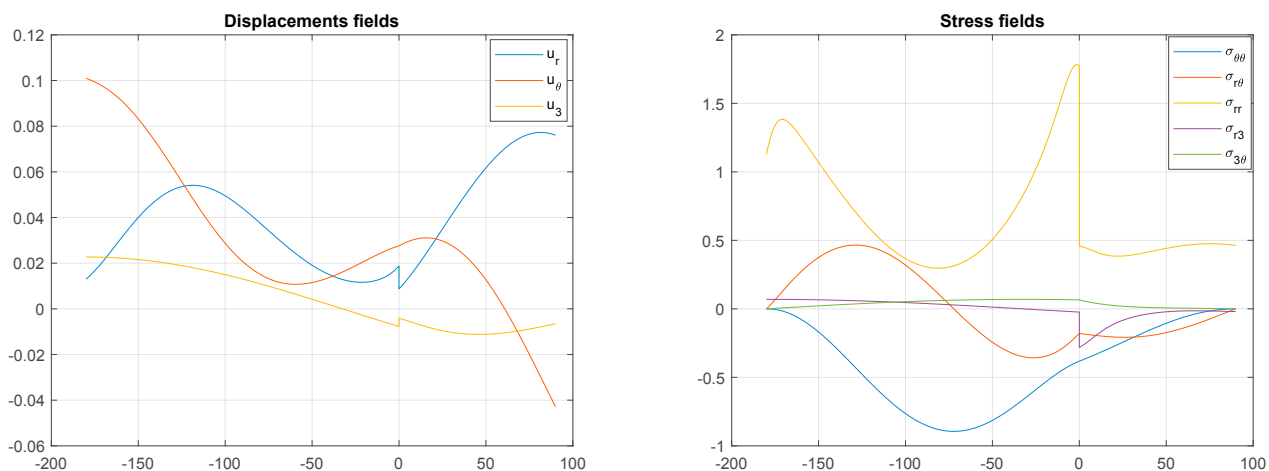
Fig. 6. Displacement and stress fields for a 90°-wedge sliding with a friction coefficient 0.5 over a semi-plane. Material B is used in both wedges. (a) Displacements, (b) Stresses.

Acknowledgements

References

Barroso, A., Mantič, V., París, F., 2003. Singularity analysis of anisotropic multimaterial corners. International Journal of Fracture 119, 1–23.

García, I., Leguillon, D., 2012. Mixed-mode crack initiation at a v-notch in presence of an adhesive joint. International Journal of Solids and Structures 49, 2138–2149.

Herrera-Garrido, M., Mantič, V., Barroso, A., 2022. A powerful matrix formalism for stress singularities in anisotropic multi-material corners. homogeneous (orthogonal) boundary and interface conditions. Theoretical and Applied Fracture Mechanics 119, 103271.

Hwu, C., 2021. Anisotropic Elasticity with Matlab. Springer, Cham.

Leguillon, D., Sanchez-Palencia, E., 1987. Computation of Singular Solutions in Elliptic Problems and Elasticity. Masson, Paris.

Mantič, V., Barroso, A., París, F., 2014. Singular elastic solutions in anisotropic multimaterial corners. Applications to composites, in: Mantič, V. (Ed.), Mathematical Methods and Models in Composites. Imperial College Press, pp. 425–495.

Mantič, V., París, F., Berger, J., 2003. Singularities in 2D anisotropic potential problems in multi-material corners. Real variable approach. International Journal of Solids and Structures 40, 5197–5218.

Mantič, V., París, F., Cañas, J., 1997. Stress singularities in 2D orthotropic corners. International Journal of Fracture 83, 67–90.

Muller, D.E., 1956. A method for solving algebraic equations using an automatic computer. Mathematical Tables and Other Aids to Computation 10, 208–215.

Stroh, A.N., 1958. Dislocations and cracks in anisotropic elasticity. The Philosophical Magazine: A Journal of Theoretical Experimental and Applied Physics 3, 625–646.

Stroh, A.N., 1962. Steady state problems in anisotropic elasticity. Journal of Mathematics and Physics 41, 77–103.

Ting, T.C.T., 1996. Anisotropic Elasticity: Theory and Applications. Oxford University Press, New York.

Ting, T.C.T., 1997. Stress singularities at the tip of interfaces in polycrystals, in: Rossmanith, H.P. (Ed.), Damage and Failure of Interfaces. Balkema Publishers, Rotterdam, pp. 75–82.

Yosibash, Z., 2012. Singularities in Elliptic Boundary Value Problems and Elasticity and Their Connection with Failure Initiation. Springer, New York.